Sensitivity Study for Improved Magnetic Induction Tomography (MIT) Coil System

Ziyi Zhang[1,2], Hengdong Lei[1,2], Peiguo Liu[2], Dongming Zhou[2]
[1] College of Science, National University of Defense Technology, Changsha, Hunan 410073, China
[2] College of Electronic Science and Engineering, National University of Defense Technology, Changsha, Hunan 410073, China
E-mail: ziyizhang@nudt.edu.cn

***Abstract*-The improved magnetic induction tomography (MIT) coil system which consists of the two-arm Archimedean spiral coil (TAASC) as excitation coil and the solenoid as receiver coil has much better performance in coil system sensitivity than the conventional MIT coil system which uses the solenoids as excitation coil and receiver coil. In this paper the theoretical sensitivity property for improved MIT coil system are studied fully. The magnetic fields produced by TAASC and solenoid are derived approximately based on the Biot-Savart law. The relations between the coil system sensitivity and the parameters (amplitude of excitation current, maximum outer radius and number of turns of TAASC, and number of turns and length of solenoid) of coil system are calculated. The results show that the sensitivity for improved MIT coil system is proportional to the number of turns of solenoid and electric current of TAASC, and can be improved with the increase of maximum outer radius of TAASC and radius of solenoid. The sensitivity is decreased as the length of solenoid increasing, and not significantly associated with the number of turns of TAASC.**

***Keywords*-Magnetic induction tomography (MIT), biological tissues, coli system sensitivity, two-arm Archimedean spiral coil (TAASC).**

I. INTRODUCTION

Magnetic induction tomography (MIT) is an emerging imaging method to reconstruct the distribution of electrical conductivity within biological tissues. Compared with the earlier electrical impedance tomography (EIT) technique, MIT has a definite advantage of non-contact, and hence is more suitable for medical applications such as the haemorrhagic cerebral stroke or brain oedema diagnosis [1].

The design of coil system is much important for MIT, which can strongly affect the sensitivity of measurement signal [2]–[4]. A typical MIT coil system includes an array of excitation coils and an array of receiver coils. As illustrated in Fig. 1, the excitation coil carrying a harmonic current I emits a primary excitation magnetic field B_0, and then a primary voltage V_0 is sensed in the receiver coil. With the action of B_0, the eddy current can be induced due to the electrically conductive object and a secondary magnetic field perturbation ΔB is produced, causing a secondary voltage perturbation ΔV sensed in the receiver coil. ΔV is of our interest, which contains the information about the electrical conductivity σ of object. Unfortunately, because the values of σ for human tissues are usually small, ΔV can be very weak in comparison with V_0, meaning low coil system sensitivity [1], [3].

The solenoid is the commonly used type of excitation coil and receiver coil in MIT coil system [5]–[8]. However, our recent study shows that this conventional MIT coil system has a low sensitivity for measuring the change of σ inside biological tissues compared to the improved MIT coil system with the two-arm Archimedean spiral coil (TAASC) as excitation coil and the solenoid as receiver coil [9]. This paper aims to investigate the sensitivity property for our improved MIT coil system comprehensively. The expressions for x, y and z component of the magnetic fields produced by TAASC and solenoid are derived approximately based on the Biot-Savart law, and then the coil system sensitivity is obtained. The maximum coil system sensitivity is tested at different amplitudes of the excitation current, different radiuses and numbers of turns of the TAASC and the solenoid, and different length of the solenoid via the MATLAB tool.

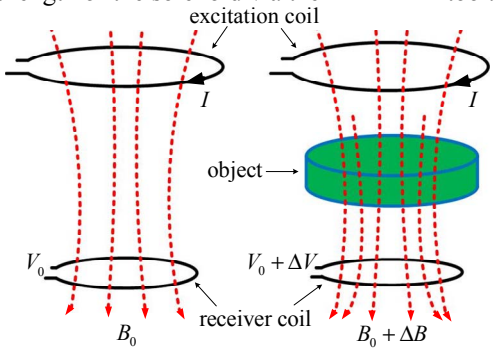

Figure 1. Schematic diagram for principle of MIT

II. METHODS

A. Model for Improved MIT Coil System

Fig. 2 shows the model for improved MIT coil system. In this model the excitation coil is a two-arm Archimedean spiral coil (TAASC) and the receiver coil is a solenoid. The TAASC is constructed by two opposite Archimedean planar spirals connected at its center. For a TAASC placed in the x-y plane with its center at the origin, the equation in polar coordinate system for it is

$$\begin{cases} L_1 : r_1 = \dfrac{r_0}{2n\pi}\varphi_1 & 0 \le \varphi_1 \le 2n\pi \\ L_2 : r_2 = \dfrac{r_0}{2n\pi}(\varphi_2 - \pi) & \pi \le \varphi_2 \le (2n+1)\pi \end{cases} \quad (1)$$

where r_0 and n are the maximum outer radius and the number of turns of TAASC, respectively [9], [10].

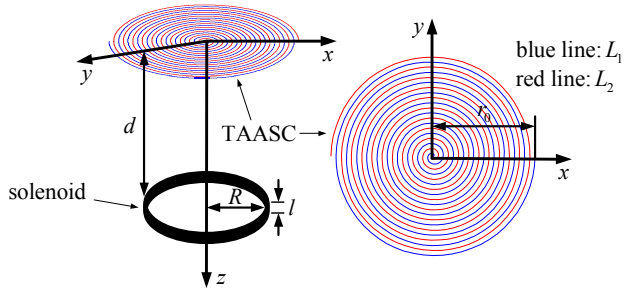

Figure 2. Model for improved MIT coil system.

B. Sensitivity Calculation in MIT Coil System

In MIT coil system, the sensitivity S is usually defined as

$$S = \frac{\Delta V}{I \Delta \kappa} \tag{2}$$

where $\kappa = \sigma + j\omega\varepsilon_0\varepsilon_r$ is the complex electrical conductivity of perturbing object and $\Delta\kappa$ represents the change of κ. According to the extensive Geselowitz relationship the coil system sensitivity S can be calculated strictly, while it is a complicated and time-consuming work [11]. However, for an isolated perturbation in the empty space S can be expressed briefly based on the reciprocity theorem as

$$S = kB_1 \cdot B_2 \tag{3}$$

where B_1 and B_2 are the magnetic fields produced by excitation coil and receiver coil respectively, and k is a constant factor only related to the perturbation characteristics [12]. Due to the unknown k, only a scaled sensitivity map could be obtained for the improved MIT coil system, but it can still reflect the sensitivity property accurately.

C. Magnetic Field Expressions for TAASC and Solenoid

For MIT the frequency of electric current in the excitation coil is generally less than 10 MHz. Therefore, the dimension of excitation coil could be very small in comparison with the wavelength of electromagnetic wave emitted by the excitation coil, and the electromagnetic field produced by the excitation coil could be treated as the static field in the region not far away from the excitation coil. According to the Biot-Savart law, for the TAASC in Fig. 2 when the excitation current I_1 in it is low-frequency, its three components of magnetic field B_1 at arbitrary point (x, y, z) in the empty space are

$$B_{1x} = p\left(\int_0^{2n\pi} \frac{(\sin\varphi_1 + \varphi_1\cos\varphi_1)z}{((x - q\varphi_1\cos\varphi_1)^2 + (y - q\varphi_1\sin\varphi_1)^2 + z^2)^{3/2}} d\varphi_1 + \int_0^{2n\pi} \frac{(\sin\varphi_2 + \varphi_2\cos\varphi_2)z}{((x + q\varphi_2\cos\varphi_2)^2 + (y + q\varphi_2\sin\varphi_2)^2 + z^2)^{3/2}} d\varphi_2\right) \tag{4}$$

$$B_{1y} = p\left(\int_0^{2n\pi} \frac{-(\cos\varphi_1 - \varphi_1\sin\varphi_1)z}{((x - q\varphi_1\cos\varphi_1)^2 + (y - q\varphi_1\sin\varphi_1)^2 + z^2)^{3/2}} d\varphi_1 + \int_0^{2n\pi} \frac{-(\cos\varphi_2 - \varphi_2\sin\varphi_2)z}{((x + q\varphi_2\cos\varphi_2)^2 + (y + q\varphi_2\sin\varphi_2)^2 + z^2)^{3/2}} d\varphi_2\right) \tag{5}$$

$$B_{1z} = p\left[\int_0^{2n\pi}\left(\frac{(\cos\varphi_1 - \varphi_1\sin\varphi_1)(y - q\varphi_1\sin\varphi_1)}{((x - q\varphi_1\cos\varphi_1)^2 + (y - q\varphi_1\sin\varphi_1)^2 + z^2)^{3/2}} - \frac{(\sin\varphi_1 + \varphi_1\cos\varphi_1)(x - q\varphi_1\cos\varphi_1)}{((x - q\varphi_1\cos\varphi_1)^2 + (y - q\varphi_1\sin\varphi_1)^2 + z^2)^{3/2}}\right) d\varphi_1 + \int_0^{2n\pi}\left(\frac{(\cos\varphi_2 - \varphi_2\sin\varphi_2)(y + q\varphi_2\sin\varphi_2)}{((x + q\varphi_2\cos\varphi_2)^2 + (y + q\varphi_2\sin\varphi_2)^2 + z^2)^{3/2}} - \frac{(\sin\varphi_2 + \varphi_2\cos\varphi_2)(x + q\varphi_2\cos\varphi_2)}{((x + q\varphi_2\cos\varphi_2)^2 + (y + q\varphi_2\sin\varphi_2)^2 + z^2)^{3/2}}\right) d\varphi_2\right] \tag{6}$$

where $p = \mu_0 r_0 I_1 / 8\pi^2 n$ and $q = r_0 / 2n\pi$.

If a solenoid with radius R, length l, number of turns N and electric current I_2 is placed at the position in Fig. 2, the magnetic fields produced by it can be derived similarly based on the Biot-Savart law as

$$B_{2x} = m\int_0^{2\pi} d\theta \int_0^{l} \frac{\cos\theta(Z - t)}{((x - R\cos\theta)^2 + (y - R\sin\theta)^2 + (Z - t)^2)^{3/2}} dt \tag{7}$$

$$B_{2y} = m\int_0^{2\pi} d\theta \int_0^{l} \frac{\sin\theta(Z - t)}{((x - R\cos\theta)^2 + (y - R\sin\theta)^2 + (Z - t)^2)^{3/2}} dt \tag{8}$$

$$B_{2z} = m\int_0^{2\pi} d\theta \int_0^{l} \frac{R - x\cos\theta - y\sin\theta}{((x - R\cos\theta)^2 + (y - R\sin\theta)^2 + (Z - t)^2)^{3/2}} dt \tag{9}$$

where $m = \mu_0 N I_2 R / 4\pi l$ and $Z = z - d$.

III. Results

A. Normalized Sensitivity Map for Reference Coil System

The improved MIT coil system which is used as a reference is based on Fig. 2. The values of related parameters for the reference coil system are listed in Table I. The calculation region is in the plane $x = 0$ with -100 mm $\le y \le 100$ mm and 10 mm $\le z \le 210$ mm. Fig. 3 shows the normalized sensitivity map for the reference coil system. The maximum sensitivity appears at the point $x = 0$, $y = 20$ mm, $z = 210$ mm.

TABLE I
VALUES OF PARAMETERS FOR REFERENCE COIL SYSTEM

Parameters	I_1	n	r_0	N	R	l	d
Values	1 A	1	50 mm	1	20 mm	10 mm	220 mm

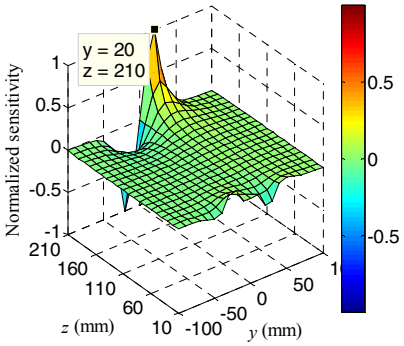

Figure 3. Normalized sensitivity map for reference coil system.

B. *Maximum Sensitivity versus Number of Turns of TAASC and Solenoid*

Fig. 4 shows the scaled maximum sensitivity versus the number of turns n of TAASC and N of solenoid. The maximum sensitivity is scaled to the maximum sensitivity of reference coil system. The variation range for n is 1 to 10 and for N is 5 to 50. In the process of changing n, the maximum sensitivity point is $x = 0$, $y = 20$ mm, $z = 210$ mm when n is 2 to 6 while at the position $x = 0$, $y = -20$ mm, $z = 210$ mm when n is 7 to 10. However, the maximum sensitivity is always at the position $x = 0$, $y = 20$ mm, $z = 210$ mm when changing N in the given range.

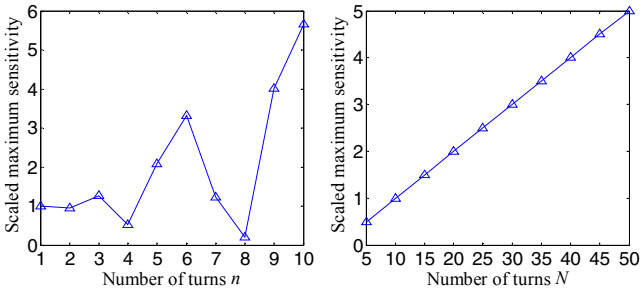

(a) (b)

Figure 4. Scaled maximum sensitivity versus number of turns n (a) of TAASC and N (b) of Solenoid.

C. *Maximum Sensitivity versus Maximum Outer Radius of TAASC and Radius of Solenoid*

Fig. 5 shows the scaled maximum sensitivity versus the maximum outer radius r_0 of TAASC and radius R of solenoid. The maximum sensitivity is scaled to the maximum sensitivity of reference coil system. The change range for r_0 and R is both 10 mm to 100 mm. The maximum sensitivity is at the position $x = 0$, $y = 20$ mm, $z = 210$ mm when changing r_0 in the given range. For the parameter R, the maximum sensitivity is obtained at the point with x-coordinate 0, z-coordinate 210 mm, and y-coordinate listed in Table II.

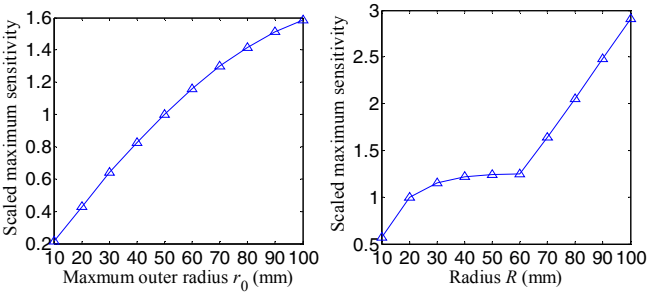

(a) (b)

Figure 5. Scaled maximum sensitivity versus maximum outer radius r_0 (a) of TAASC and radius R (b) of solenoid.

TABLE II
Y-COORDINATE OF MAXIMUM SENSITIVITY POINT VERSUS RADIUS OF SOLENOID IN THE CALCULATION REGION

R	10 mm	20 mm	30 mm	40 mm	50 mm
y-coordinate	10 mm	20 mm	30 mm	40 mm	50 mm
R	60 mm	70 mm	80 mm	90 mm	100 mm
y-coordinate	–20 mm	–20 mm	–20 mm	–20 mm	–20 mm

D. *Maximum Sensitivity versus Electric Current of TAASC and Length of Solenoid*

Fig. 6 shows the scaled maximum sensitivity versus the electric current I_1 of TAASC and the length l of solenoid. The maximum sensitivity is scaled to the maximum sensitivity of reference coil system. The change range for I_1 is 0.2 A to 2 A and for l is 5 mm to 50 mm. The maximum sensitivity is at the position $x = 0$, $y = 20$ mm, $z = 210$ mm when changing I_1 and l in the given range.

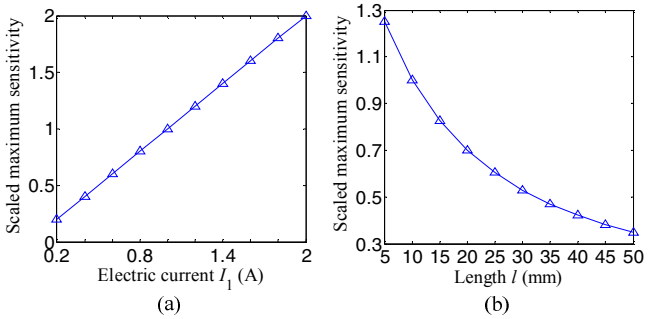

(a) (b)

Figure 6. Scaled maximum sensitivity versus electric current I_1 (a) of TAASC and length l (b) of solenoid.

IV. DISCUSSIONS AND CONCLUSIONS

In the improved MIT coil system, the sensitivity is a quantity related to the position of perturbation. For the reference coil system, its sensitivity map is anti-symmetric about the plane $y = 0$ and the maximum value appears at the point $x = 0$, $y = 20$ mm, $z = 210$ mm in the calculation region, as shown in Fig. 3.

It can be seen from Fig. 4 that the sensitivity for improved MIT coil system does not specifically relate to the number of turns of TAASC, but is proportional to the number of turns of solenoid. The position of maximum sensitivity is unfixed with the number of turns of TAASC increasing, and yet invariable no matter how the number of turns of solenoid changes.

In Fig. 5, the coil system sensitivity can be improved by increasing the maximum outer radius of TAASC or the radius of solenoid. The position of maximum sensitivity is unaltered with the increase of maximum outer radius of TAASC. However, the y-coordinate of maximum sensitivity point is variable when the radius of solenoid increases, as show in Table II.

The coil system sensitivity is proportional to the electric current of solenoid, and decreases as the length of solenoid increases, as shown in Fig. 6. The position of maximum sensitivity is unfixed regardless of the change for electric current of TAASC and length of solenoid.

In conclusion, the sensitivity for improved MIT coil system has its maximum value in the region of interest, and the perturbing object ought to be placed near the maximum sensitivity point. The coil system sensitivity could be improved by increasing the maximum outer radius of TAASC, electrical current of TAASC, number of turns of solenoid and radius of solenoid. For the actual design of improved MIT coil system, all the parameters should be considered synthetically in order to make the coil system sensitivity optimum.

ACKNOWLEDGMENT

This work was supported by the Specialized Research Fund for the Doctoral Program of Higher Education of China (No. 20114307110022) from Ministry of Education of the People's Republic of China.

REFERENCES

[1] H.-Y. Wei and M. Soleimani, "Electromagnetic tomography for medical and industrial applications: challenges and opportunities," *Proc. IEEE*, vol. 101, pp. 27–46, Mar. 2013.

[2] A. J. Peyton, Z. Z. Yu, G. Lyon, S. Al-Zeibak, J. Ferreira, J. Velez, F. Linhares, A. R. Borges, H. L. Xiong, N. H. Saunders and M. S. Beck, "An overview of electromagnetic inductance tomography: description of three different systems," *Meas. Sci. Technol.*, vol. 7, pp. 261–271, Mar. 1996.

[3] H. Griffiths, "Magnetic induction tomography," *Meas. Sci. Technol.*, vol. 12, pp. 1126–1131, Aug. 2001.

[4] S. Watson, C. H. Igney, O. Dössel, R. J. Williams and H. Griffiths, "A comparison of sensors for minimizing the primary signal in planar-array magnetic induction tomography," *Physiol. Meas.*, vol. 26, pp. S319–S331, Apr. 2005.

[5] A. Korjenevsky, V. Cherepenin and S. Sapetsky, "Magnetic induction tomography: experimental realization," *Physiol. Meas.*, vol. 21, pp. 89–94, Feb. 2000.

[6] S. Watson, R. J. Williams, W. Gough and H. Griffiths, "A magnetic induction tomography system for samples with conductivities below 10 S m^{-1}," *Meas. Sci. Technol.*, vol. 19, pp. 045501, Apr. 2008.

[7] M. Vauhkonen, M. Hamsch and C. H. Igney, "A measurement system and image reconstruction in magnetic induction tomography," *Physiol. Meas*, vol. 29, pp. S445–S454, Jun. 2008.

[8] H.-Y. Wei and M. Soleimani, "Hardware and software design for a National Instrument-based magnetic induction tomography system for prospective biomedical applications," *physiol. Meas.*, vol. 33, pp. 863–879, May 2012.

[9] Z. Zhang, P. Liu, D. Zhou and H. Lei, "Biomedical magnetic induction using two-arm Archimedean spiral coil: a feasibility study," unpublished.

[10] Z. Zhang, P. Liu, L. Ding and L. Zhang, "A new type of excitation coil for measurement of liver iron overload by magnetic induction method," in *Proc. 5th Int. Conf. BioMedical Engineering and Informatics*, Chongqing, China, 2012, pp. 679–683.

[11] R. J. Mortarelli, "A generalization of the Geselowitz relationship useful in impedance plethysmographic field calculations," *IEEE Trans. Biomedical Engineering*, vol. 27, pp. 665–667, Nov. 1980.

[12] J. Rosell, R. Casañas and H. Scharfetter, "Sensitivity maps and system requirements for magnetic induction tomography using a planar gradiometer," *Physiol. Meas.*, vol. 22, pp. 121–130, Feb. 2001.